Drone Classification and Localization Using Micro-Doppler Signature with Low-Frequency Signal

Yingxiang Sun, Hua Fu, Samith Abeywickrama, Lahiru Jayasinghe, Chau Yuen, Jiajia Chen
Engineering Product Development Pillar, Singapore University of Technology and Design, Singapore
Email: yingxiang_sun@mymail.sutd.edu.sg, hua_fu@sutd.edu.sg, tharindu@mymail.sutd.edu.sg,
{aruna_jayasinghe, yuenchau, jiajia_chen}@sutd.edu.sg

***Abstract*—Security issues have been raising accompanied by the popularization of drone in recent years. To address these issues, drone detection, classification and localization techniques are needed to be developed. In this paper, we propose a new approach for drone classification and localization. After obtaining micro-Doppler signature generated from drone propeller rotation, dimension reduction is carried out for feature extraction. Finally, features are fed into four different classifiers. We conduct practical experiments with radio frequency signal at low-frequency band. The experimental results show that we effectively realize drone classification as well as localization with good robustness.**

***Keywords*—Micro-Doppler signature, drone classification, drone localization, low frequency**

I. INTRODUCTION

In the past few years, drone has been widely used for aerial photography, express delivery, security monitoring, power line inspection, rescue mission, and so on. However, unsafe operations and even criminal offenses [1] pose serious threats to aviation safety and public security. To cope with these threats, it is necessary to develop detection, classification, and localization technologies for drone.

Drones can be roughly categorized into two groups: those themselves emit a signal and those themselves do not emit any signal. In this paper, we focus on the latter group. For the latter group, different sensors can be adopted to detect drones. Among these sensors, radar has advantages in three aspects. Compared with electro-optical sensor and infrared sensor, radar can operate at all-light and all-weather environments. Moreover, radar performs better at spatial searching while it can provide the speed and range of the target. In addition, unlike acoustic sensor, radar is unaffected by high-level acoustic noise outdoors.

However, as drones fly at low altitude with slow speed and small radar cross-section, it is difficult for conventional radar to detect, classify and localize them. To address this problem, micro-Doppler effect [2] can be utilized. To date, many efforts have been made to obtain and analyze micro-Doppler signature (MDS). Two types of presentations are commonly used to represent MDS, viz, time-frequency spectrogram [3]-[7] and time-velocity diagram [8]-[11]. Diverse features have been extracted from MDS, including received power feature [6], bicoherence feature [7], singular value decomposition feature [10], and physical feature [11]. In addition to feature extraction, some works [6], [7], [10]-[12] also involve drone classification.

Although the above great works have been done, there are still two more challenges to be addressed. The first issue is to realize drone classification in low frequency band. Compared with high-frequency signal, low-frequency signal can propagate further, enabling both short-distance and long-distance detection for drone. However, the MDS of drone becomes blurred at low-frequency band, making classification difficult. So far, only a few works [4], [13], [14] operate at low frequency such as UHF band (300–1000 MHz) and L band (1–2 GHz) according to IEEE standard 521–2002[15], merely analyzing MDS without classification. Moreover, [13] and [14] present results of helicopter rather than drone. The second issue is to localize drone using MDS. Up to now, a few attempts such as [16] and [17] have been made to localize drone, however, they use conventional radar location methods rather than using MDS. Although MDS is employed by the approach proposed in [16], it is only used to discriminate drone from clutter. To the best of our knowledge, drone localization using MDS has not been done.

The main contributions of this paper can be summarized as follows:

1) We realize drone classification using MDS by practical experiments with UHF band radio frequency signal. Although the experiments are conducted at a short range due to limited experimental instruments at hand, the validity of our proposed approach applied in the case of long distance still can be verified.
2) On top of classification, we further realize drone localization using MDS by machine learning approach while relative work has not been done yet.

II. OVERVIEW OF THE PROPOSED APPROACH

The echo signal from drone is corrupted by noise component that consists of ambient noise from environment and thermal noise caused by measuring instrument. Moreover, besides micro-Doppler component generated from micromotion (i.e. propeller rotation), the echo signal also contains bulk component due to bulk motion and clutter component resulted from clutter reflection. After receiving the echo signal, to accomplish drone classification and localization, we propose an approach consisting of three stages as below.

Since micro-Doppler component is faint, other components can easily mask it, leading to severe performance degradation of classification and localization. Therefore, in the first stage,

the echo signal is processed to contain only the micro-Doppler component. To effectively remove other components at low-frequency band, spectral subtraction method [18] is first used to reduce noise. Then, bulk motion component is removed by setting the Doppler shifted carrier frequency to be zero. Finally, empirical mode decomposition (EMD) method [19] is employed to further eliminate clutter component and remove noise.

In the second stage, features are extracted from the obtained MDS. Short-time Fourier transform (STFT) is carried out to obtain the time-frequency distribution (i.e. spectrogram) that represents MDS. Since MDS contains unreliable information, it is not suitable to be directly used as feature. Therefore, to remove unreliable information, features are extracted from MDS by principle component analysis (PCA) [20], a dimension reduction technique.

In the third stage, training data and ground truth will be used to train classifier. Then, extracted features from testing data are fed into classifier to accomplish drone classification and localization.

The flow chart of the proposed approach is depicted in Fig. 1. Each stage of the proposed approach will be presented in detail in Section III.

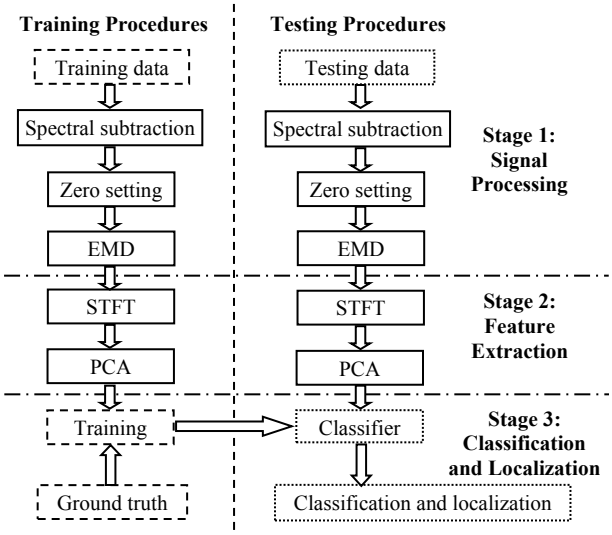

Fig. 1. Flow chart of drone classification and localization

III. The Proposed Approach

A. Signal Processing

Spectral subtraction method can effectively achieve noise reduction through subtracting noise spectrum from noisy echo signal spectrum. Assume that the sampled noisy echo signal $x(m)$ in discrete time domain can be expressed as

$$x(m) = s(m) + n(m), \tag{1}$$

where $s(m)$ is caused by bulk motion, micromotion and clutter, $n(m)$ is noise component, m is the discrete time index. Eq. (1) can be rewritten in frequency domain as

$$X(f) = S(f) + N(f), \tag{2}$$

where $X(f)$, $S(f)$, and $N(f)$ are the corresponding Fourier transforms. Next, the time-averaged noise magnitude spectrum $\overline{|N(f)|}$ can be subtracted from the noisy signal magnitude spectrum as

$$\left|\hat{S}(f)\right| = |X(f)| - \overline{|N(f)|}, \tag{3}$$

where $|\hat{S}(f)|$ is the estimated magnitude spectrum of $s(m)$.

In terms of frequency spectrum of echo signal, the Doppler shifted carrier frequency corresponds to bulk motion component while the side-band Doppler frequency around the Doppler shifted carrier frequency corresponds to micro-Doppler component. In the remaining frequency spectrum $\hat{S}(f)$ after spectral subtraction, to remove bulk motion component, we set the Doppler shifted carrier frequency to be zero. After that, we obtain frequency spectrum $E(f)$.

EMD is a time-frequency analysis method which can decompose any given signal into a set of frequency ordered intrinsic mode functions (IMFs). These IMFs are orthogonal to each other and they are in time-domain with the same length as the original signal. For each successive IMF, the lower-indexed one contains the higher frequency oscillations. The IMFs shall satisfy two requirements: for each IMF, (i) the number of local extrema differs from the number of zero-crossings at most by one; (ii) the average of the envelop shall be zero.

Assume $e(m)$ is the time domain form of $E(f)$, firstly, its upper envelop $e_{\max}(m)$ and lower envelop $e_{\min}(m)$ are identified. The first IMF $imf_1(m)$ can be obtained by computing the mean of these two envelopes:

$$imf_1(m) = \frac{e_{\max}(m) + e_{\min}(m)}{2}. \tag{4}$$

Then, we subtract $imf_1(m)$ from $e(m)$ and compute the residue $r_1(m)$. This procedure will be repeated until no more than two extrema existing in the residue and therefore all IMFs are extracted. The final residue $r(m)$ stands for the general trend of $e(m)$. Thus, $e(m)$ can be decomposed as

$$e(m) = \sum_{i=1}^{L} imf_i(m) + r(m), \tag{5}$$

where L denotes the total number of IMFs. The micro-Doppler component $y(m)$ can be obtained by summing IMFs corresponding to micro-Doppler frequency, i.e. $y(m) = \sum imf_j(m)$, where $j \in [1, L]$.

B. Feature Extraction

The time-frequency MDS contains information of micro-Doppler shift which can be computed as

$$f_{\max} = \frac{2fv_{tip}}{c}\cos\alpha\cos\beta, \tag{6}$$

where f_{max} is the maximum micro-Doppler shift, f is the carrier frequency, $v_{tip}=2\pi L\Omega$ is the velocity of blade tip, where L is the length of blade and Ω is the rotation rate, c is velocity of light, α and β are azimuth angle and elevation angle in terms of radar line-of-site respectively. As micro-Doppler shift varies along with L, Ω, α, and β, the clues of drone type and location are implied in MDS. This provides the potential to realize drone classification as well as localization by feature extracted from MDS.

We use STFT to obtain the time-frequency distribution, i.e. spectrogram, to represent MDS. To implement STFT, $y(m)$ is segmented by overlapping sliding frames $w(u)$ with length U.

Thus, we obtain a series of segmented signals $y_v(u)$, where v=0, 1, …, V–1. By performing Fourier transform to $y_v(u)$, time-frequency representation $F_{TF}(v, h)$ can be obtained as

$$F_{TF}(v,h)=\sum_{u=0}^{U-1} y_v(u)\exp\left(-j2\pi\frac{uh}{U}\right),\quad h=0,1,...,U-1. \tag{7}$$

The magnitude forms spectrogram $F(v, h)$ of size V × U as

$$F(v,h)=|F_{TF}(v,h)|^2. \tag{8}$$

PCA is a dimension reduction technique which casts data into a linear subspace of lower dimension through a linear mapping A. Thus, the low-dimension data can represent the original high-dimension data. PCA can remove unreliable information from MDS meanwhile lower computational complexity of subsequent classification and localization. Assume the covariance matrix of spectrogram F is D, A can be obtained by the d principle eigenvectors of D. Therefore, PCA solves the eigenproblem for the d principal eigenvalues λ:

$$DA=\lambda A. \tag{9}$$

The representation Z of F can be computed by

$$Z=FA. \tag{10}$$

By aligning the d columns to be one column, we can obtain the feature B, which is the input of classifier.

C. Classification and Localization

Assume that there are Q locations of interest and the drone is located in one of them. We aim to use a classifier to discriminate which location the drone is from among all the Q candidates. Therefore, the localization accuracy is measured in a percentage. Assume that there are P different types of drones, we can obtain Q×P classes in total, in which the information of both drone type and location are implied. In this case, drone classification and localization can be realized simultaneously by a classifier. Four widely used classifiers [21] are employed, namely, k-nearest neighbor (KNN), random forest (RF), naive Bayes (NB), and support vector machine (SVM).

KNN is an instance-based learning classifier, realizing classification according to the distances among different input samples, i.e. features. Assume that there are a total number of c classes, i.e. C_i with $i \in [1, c]$. The k nearest samples to feature B will be found, and then the most frequent class C_i of these k samples will be assigned to B.

RF classifier uses a series of decision trees to classify input features into different classes. A random subset of the features will be chosen for each possible split. For feature B, the forest chooses the class C_i owning the most votes according to the results of each tree.

NB is a probabilistic classifier based on conditional probability model. Assume that the features are conditionally independent given the class label, we can obtain a joint conditional probability for each feature. By applying the Bayes rule, the class C_i with the highest probability will be chosen for feature B.

In terms of SVM classifier, it is originally designed for binary classification using a hyperplane with the large margin principle. By using one-versus-one coding design, $c(c–1)/2$ SVMs can be combined to form a multi-class classifier. Therefore, feature B can be classified into the class C_i which has the highest number of votes.

D. Computational Complexity

In signal processing stage, the complexity of spectral subtraction is $O(t_1 \times n_1 \times \log n_1)$, where t_1 is the total number of frame, n_1 is the length of fast Fourier transform. For EMD, its complexity is $O(n_s \times n_{imf} \times \log n_{imf})$, where n_s is the number of siftings, n_{imf} is the length of each IMF.

In the feature extraction step, the complexity of STFT is $O(t_2 \times n_2 \times \log n_2)$, where t_2 is the total number of frame, n_2 is the length of fast Fourier transform. PCA costs $O(n_2^2 \times n_o + n_2^3)$ complexity, as the input vector is in the form of n_o columns with n_2 dimensions.

In the third stage, $O(n_t \times n_d + n_t \times k)$ complexity is cost for KNN classifier, where n_t is the number of training samples, n_d is dimension of each feature, k is the number of nearest samples. For RF classifier, its complexity is $O(M \times K \times n_t \times \log^2 n_t)$, where M denotes the number of randomized trees, K denotes number of variables randomly drawn at each node. For NB classifier, $O(n_t \times n_d + c \times n_d + n_t \times n_d \times c)$ complexity is cost, where c is the number of classes. For SVM classifier, the complexity is $O(n_t \times c^2)$.

IV. Experimental Results

A. Experimental Setup

The experiments are conducted in campus center hall, where the setup is shown as in Fig. 2.

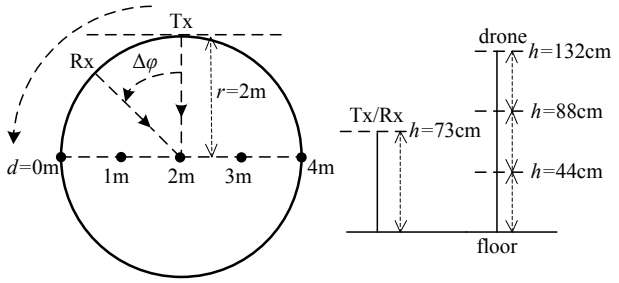

(a)

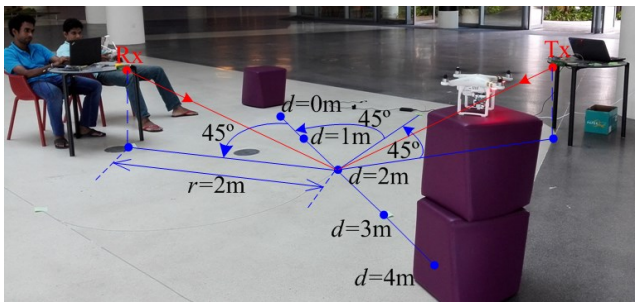

(b)

Fig. 2. Experimental setup

Due to limited experimental instruments at hand, we use a pair of low power continuous wave transmitter and receiver to generate UHF single tone signal and receive echo signal. Therefore, the experimental operating distance is limited in a short range. However, even with short-distance experiments, the validity of proposed method which can be applied for long-distance still can be verified. The long-distance experiments will be carried out in the future. The carrier frequency is

centered at 915*M*Hz with 2*k*Hz bandwidth while the transmitting power is with an upper limit of 100*m*W. The sample rate for received signal is 32*k*Hz/s. Both the transmitter and the receiver are placed on a circle with radius r=2m, pointing to the center of the circle at 73cm height, operating with beamwidth of 45˚. The transmitter is placed at a fixed position while the receiver is placed at three different angles away from the transmitter in anticlockwise direction, successively with interval of $\Delta\varphi$ = 45˚, 90˚, and 135˚. The drone used for experiments is a carbon fiber quadcopter by DJI corporation, which is 16cm high. When only 1 propeller is retained while all other 3 propellers are removed, the drone can be treated as a micro-helicopter. For each angle, the measurements with micro-helicopter and quadcopter are carried out at four different positions along the diameter, viz, d=1m, 2m, 3m, and 4m. At each position, the drone is placed at three different heights, i.e. h=44cm, 88cm, and 132 cm.

B. Validation of MDS Feature Extraction

The time-frequency spectrogram is shown as in Fig. 3, where d=2m, h=132cm. Figs. 3(a), (c), and (e) show the results of micro-helicopter when $\Delta\varphi$ = 45˚, 90˚, and 135˚ respectively. Similarly, results of quadcopter are illustrated in Figs. 3(b), (d), and (f), which are much distinctive from those of micro-helicopter. From Fig. 3(a), it can be observed that the micro-Doppler frequency varies as sinusoidal curve with 61 periods in 1s with maximum value around 260Hz. As the radius of drone propeller is 0.12m while cosα=1 and cosβ=0.936 can be calculated, we can estimate the maximum micro-Doppler frequency according to Eq. (6). Thus, the estimated maximum micro-Doppler frequency is about 262Hz, matching the experimental results well. This shows that the validity of obtained time-frequency spectrogram. MDS varies from Fig. 3(a) to (f) with different number of propellers and different locations, validating the possibility of classification and localization using MDS.

C. Performance of Classification and Localization

According to experimental setup, there are 2 types of drone, i.e. micro-helicopter and quadcopter. As both are measured at 36 different locations, thus, there are 72 classes in total. After discarding some untrusted data, data from 31 locations of micro-helicopter and 35 locations of quadcopter are used. Hence, 66 classes are applied to the four classifiers, in which the information of both drone type and location are implied. 30 training samples and 5 testing samples are extracted from 1-second received signal for each class. For the KNN classifier, k=1 is chosen. In terms of RF classifier, 50 decision trees are created. The results of classification and localization are shown in Table I.

The accuracy of this 66-class classification and localization task achieves up to 91.2% with RF classifier while only 77.9% with KNN classifier. The results show that localization can be effectively realized, on top of drone classification. Also, the results validate the robustness of MDS features extracted from different positions. Moreover, among these 66-class results, the 31-class results solely involving micro-helicopter show that the localization accuracy of micro-helicopter stabilizes at around 95%, indicating good localization performance on top of correct classification. In contrast, the localization accuracy of quadcopter is lower, varying between 62.3% and 85.7%. The reason is that MDS is blurred at low-frequency band when multi propellers rotate simultaneously. However, good performance still can be achieved by RF classifier and NB classifier.

It is worth pointing out that the results in this paper are obtained with different radar positions. When the radar position changes, the clutter component of echo signal varies. However, as the clutter component can be effectively removed in stage 1 of our proposed approach, the slightly difference of echo signal caused by radar position can be ignored. Moreover, when new drones with different propellers appear, the new MDS features can be obtained and added into the classification and localization system.

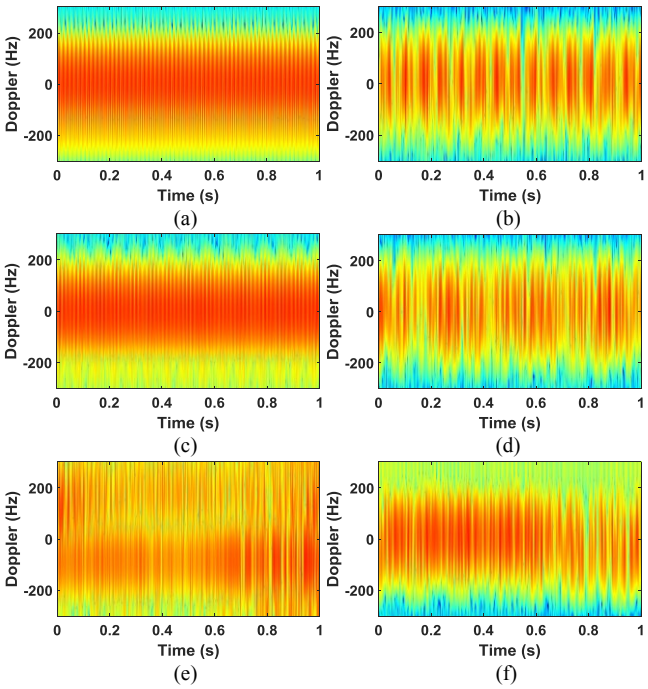

Fig. 3. Time-frequency spectrogram

Table I Results of classification and localization

Classifier	KNN	RF	NB	SVM
Accuracy(66-class, total)	77.9%	91.2%	90.0%	83.0%
Accuracy(31-class, micro-helicopter)	95.5%	97.4%	94.8%	94.8%
Accuracy(35-class, quadcopter)	62.3%	85.7%	85.7%	72.6%

V. CONCLUSIONS

In this paper, by jointly using spectral subtraction technique and EMD technique, we address the challenging problem of drone classification at low-frequency band. Moreover, by using MDS, on top of pure target classification, we further realize localization for drone, which has not been done to the best of our knowledge. The practical experimental results have shown the effectiveness and robustness of our proposed method.

REFERENCES

[1] D. Sathyamoorthy, "A review of security threats of unmanned aerial vehicles and mitigation steps," *J. Def. Secur.*, vol. 6, no. 2, pp. 81–97, Oct. 2015.

[2] V. C. Chen, F. Li, S. S. Ho, and H. Wechsler, "Micro-doppler effect in radar: Phenomenon, model, and simulation study," *IEEE Trans. Aerosp. Electron. Syst.*, vol. 42, no. 1, pp. 2–21, Jan. 2006.

[3] P. Suresh, T. Thayaparan, T. Obulesu, and K. Venkataramaniah, "Extracting micro-doppler radar signatures from rotating targets using fourier-bessel transform and time-frequency analysis," *IEEE Trans. Geosci. Remote Sens.*, vol. 52, no. 6, pp. 3204–3210, Jun. 2014.

[4] M. A. Govoni, "Micro-Doppler signal decomposition of small commercial drones," in *Proc. IEEE Radar Conf.*, Seattle, USA, May 2017, pp. 0425–0429.

[5] J. A. Nanzer and V. C. Chen, "Microwave interferometric and Doppler radar measurements of a UAV," in *Proc. IEEE Radar Conf.*, Seattle, USA, May 2017, pp. 1628–1633.

[6] M. Ritchie, F. Fioranelli, H. Borrion, and H. Griffiths, "Multistatic micro-Doppler radar feature extraction for classification of unloaded/loaded micro-drones," *IET Radar, Sonar Navig.*, vol. 11, no. 1, pp. 116–124, Jan. 2017.

[7] P. Molchanov et al., "Classification of aircraft using micro-Doppler bicoherence-based features," *IEEE Trans. Aerosp. Electron. Syst.*, vol. 50, no. 2, pp. 1455-1467, Apr. 2014.

[8] J. J. M. de Wit, R. I. A. Harmanny, G. Prémel-Cabic, "Micro-Doppler analysis of small UAVs," in *Proc. 9th Eur. Radar Conf.*, Amsterdam, Netherlands, Oct. 2012, pp. 210-213.

[9] J. J. M. de Wit, R. I. A. Harmanny, and P. Molchanov, "Radar micro-Doppler feature extraction using the singular value decomposition," in *Proc. Int. Radar Conf.*, Lille, France, Oct. 2014, pp. 1–6.

[10] P. Molchanov, R. I. A. Harmanny, J. J. M. de Wit, K. Egiazarian, and J. Astola, "Classification of small UAVs and birds by micro-Doppler signatures," *Int. J. Microw. Wirel. Technol.*, vol. 6, no. 3–4, pp. 435–444, Jun. 2014.

[11] S. Bjorklund, T. Johansson, and H. Petersson, "Target classification in perimeter protection with a micro-Doppler radar," in *Proc. 17th Int. Radar Symp.*, Krakow, Poland, May 2016, pp. 1–5.

[12] B. K. Kim, H. S. Kang, and S. O. Park, "Drone classification using convolutional neural networks with merged doppler images," *IEEE Geosci. Remote Sens. Lett.*, vol. 14, no. 1, pp. 38–42, Jan. 2017.

[13] C. Clemente and J. J. Soraghan, "Gnss-based passive bistatic radar for micro-doppler analysis of helicopter rotor blades," *IEEE Trans. Aerosp. Electron. Syst.*, vol. 50, no. 1, pp. 491–500, Jan. 2014.

[14] P. Samczyński, K. Kulpa, J. Misiurewicz, and M. K. Bączyk, "Micro-Doppler signatures of helicopters in multistatic passive radars," *IET Radar, Sonar Navig.*, vol. 9, no. 9, pp. 1276–1283, 2015.

[15] *IEEE Standard Letter Designations for Radar-Frequency Bands*, IEEE Standard 521–2002 (Revision of IEEE Std 521–1984), 2003, pp. 1–3.

[16] F. Hoffmann, M. Ritchie, F. Fioranelli, A. Charlish, and H. Griffiths, "Micro-Doppler based detection and tracking of UAVs with multistatic radar," in *Proc. IEEE Radar Conf.*, Philadelphia, USA, May 2016, pp. 1–6.

[17] M. Caris, W. Johannes, S. Stanko, N. Pohl, "Millimeter wave radar for perimeter surveillance and detection of MAVs (Micro Aerial Vehicles)," in *Proc. Int. Radar Symposium*, Dresden, Germany, June 2015, pp. 284–287.

[18] S. V. Vaseghi, Advanced digital signal processing and noise reduction, 4th edition, Wiley press, 2009.

[19] R. M. Narayanan and D. P. Fairchild, "Classification of human motions using empirical mode decomposition of human micro-Doppler signatures," *IET Radar, Sonar Navig.*, vol. 8, no. 5, pp. 425–434, Jun. 2014.

[20] A. Balleri, K. Chetty, and K. Woodbridge, "Classification of Personnel Targets by Acoustic Micro-Doppler Signatures," *IET Radar, Sonar Navig.*, vol. 5, no. 9, pp. 943–951, Dec. 2011.

[21] K. P. Murphy, Machine learning: A probabilistic perspective, MIT press, 2012.